

Iván Agudo^{1,2}, Svetlana G. Jorstad^{2,3}, Alan P. Marscher², Valeri M. Larionov^{3,4}, José L. Gómez¹, Anne Lähteenmäki⁵, Mark Gurwell⁶, Paul S. Smith⁷, Helmut Wiesemeyer⁸, Clemens Thum⁹, Jochen Heidt¹⁰

¹ Instituto de Astrofísica de Andalucía, CSIC, Apartado 3004, 18080, Granada, Spain, ² Institute for Astrophysical Research, Boston University, 725 Commonwealth Avenue, Boston, MA 02215
³ Astronomical Institute, St. Petersburg State University, Universitetskij Pr. 28, Petrodvorets, 198504 St. Petersburg, Russia, ⁴ Isaac Newton Institute of Chile, St. Petersburg Branch, St. Petersburg, Russia
⁵ Aalto University Metsähovi Radio Observatory, Metsähoviitie 114, FIN-02540 Kylmäla, Finland, ⁶ Harvard-Smithsonian Center for Astrophysics, 60 Garden St., Cambridge, MA 02138, USA
⁷ Steward Observatory, University of Arizona, Tucson, AZ 85721-0065, USA, ⁸ Institut de Radio Astronomie Millimétrique, Avenue Divina Pastora, 7, Local 20, E-18012 Granada, Spain
⁹ Institut de Radio Astronomie Millimétrique, 300 Rue de la Piscine, 38406 St. Martin d'Hères, France, ¹⁰ ZAH, Landessternwarte Heidelberg, Königstuhl, 69117 Heidelberg, Germany

Abstract: We combine the Fermi-LAT light curve of the BL Lacertae type blazar OJ287 with time-dependent multi-wavelength flux and linear polarization observations and sub-millisecond-scale polarimetric images at 7mm to locate the γ -ray emission in prominent flares in the jet of the source > 14 pc from the central black hole. This poster reproduces recently published paper: Agudo et al. (2011, ApJL, 726, L13).

Introduction

The information that γ -ray observations can provide on the physical properties of blazars, depends on where such γ -ray emission originates, which is still under intense debate.

We combine the Fermi-LAT light curve of the BL Lacertae type blazar OJ287 ($z=0.306$) with time-dependent multi-wavelength flux and linear polarization observations and 7mm ultra-high angular-resolution (~ 0.15 mas) monthly monitoring with the Very Long Baseline Array (VLBA) to resolve the innermost jet regions and to locate the γ -ray emission in prominent flares.

Our photo-polarimetric observations of OJ287 (Figs. 2 and 3) include 7mm VLBA images (Fig. 1), 3mm monitoring with the IRAM 30m Telescope, and optical (R and V bands) observations from Calar Alto, Steward, Lowell, St. Petersburg State University, and Crimean Astrophysical observatories, plus public data from Villforth et al. (2010). Our total flux light curves (Fig. 2) include the public data from Fermi-LAT (γ -rays, 0.1–200 GeV), Swift (X-rays, 0.3–10 keV), and the SMARTS program. To these, we also add light curves from the SMA at 1.3 mm and 850 μ m, from the IRAM 30m Telescope at 1.3 mm, and from the Metsähovi Observatory at 8mm. See Agudo et al. (2011) for details about the data reduction.

Results & Discussion

7 mm Jet Structure and Kinematics

We model the brightness distribution of the source at 7 mm with a small number of circular Gaussian components. Our model fits include a bright quasi-stationary feature (C1) ~ 0.2 mas from the innermost jet region (C0). The identification of C0 as the innermost jet feature is justified by the decreasing intensity westward of C1, and by the detection after 2010 March of superluminal motion of features M1 and M2 toward the west-southwest of C1 with speeds of $10.8c \pm 1.3c$ and $6.7c \pm 1.4c$, and possibly M3, which crossed C1 in 2010 October (preliminary speed of $\geq 10c$).

Flares in the C1 Jet Region at 1 mm and 7 mm

C0 and C1 typically governed the millimeter-wave evolution, of OJ287. Actually, the two most prominent 1 mm flares ever reported in OJ287 (A_{mm} and B_{mm} , see Fig. 2) took place in C1, as indicated by the correspondence of events in the 7mm light curve of C1 with those at other millimeter wavelengths.

From the angle of the jet axis to the line of sight in OJ287 (1.9° – 4.1° ; Jorstad et al. 2005; Pushkarev et al. 2009), and the mean projected separation of C1 from C0 at the time of start of A_{mm} and B_{mm} (0.23 ± 0.01 mas), we estimate that C1 is located >14pc downstream of C0, the innermost jet region detected in our images. The actual distance between the central engine in OJ287 and C1 must be even greater if C0 lies downstream of the acceleration and collimation zone (ACZ) of the jet (Jorstad et al. 2007; Marscher et al. 2008, 2010).

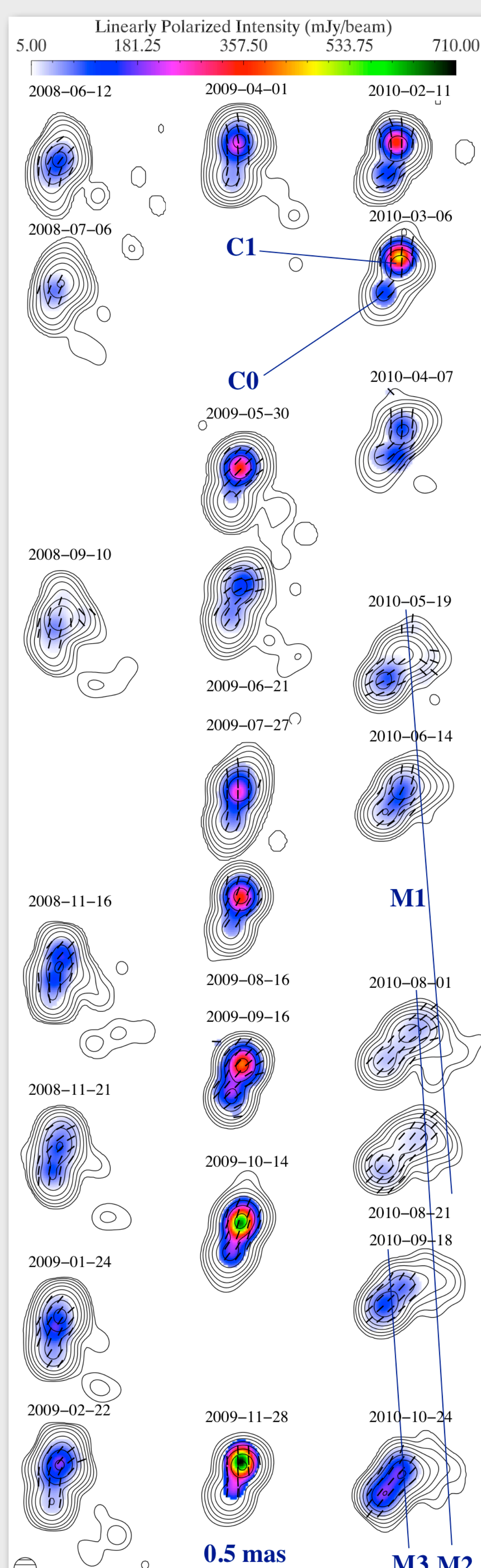


Figure 1. Sequence of 7 mm VLBA images of OJ287 in 2008–2010. Images are convolved with an FWHM = 0.15 mas circular Gaussian beam. Contour levels represent 0.2%, 0.4%, 0.8%, 1.6%, 3.2%, 6.4%, 12.8%, 25.6%, 51.2%, and 90.0% of the peak total intensity of $6.32 \text{ Jy beam}^{-1}$. The color scale indicates linearly polarized intensity, whereas superimposed line segments represent the orientation of the polarization electric-vector position angle. We adopt the standard Λ CDM cosmology with $H_0 = 71 \text{ km s}^{-1} \text{ Mpc}^{-1}$, $\Omega_M = 0.27$, and $\Omega_\Lambda = 0.73$, so that 1mas corresponds to a projected distance of 4.48 pc, and a proper motion of 1 mas yr $^{-1}$ corresponds to a superluminal speed of 19c. Reproduced from Agudo et al. (2011).

γ -Ray Flares

The two most pronounced γ -ray flares take place during the initial rising phases of A_{mm} and B_{mm} (Fig. 2). The discrete correlation function (DCF) between the γ -ray and 1mm long-term light curve (Figure 4) possesses a prominent peak at a time lag ~ -80 days (γ -ray leading). Our Monte-Carlo simulations (see Agudo et al. 2011) show that the DCF peak is significant at 99.7% confidence in all of our simulations. This confirms the correlation between B_γ and B_{mm} , the most luminous γ -ray and 1mm flares in our data. The correlation of the γ -ray and 8 mm light curves in Fig. 2 is of similarly high significance.

The optical light curves show two sharp flux increases at essentially zero time lag from A_γ and B_γ .

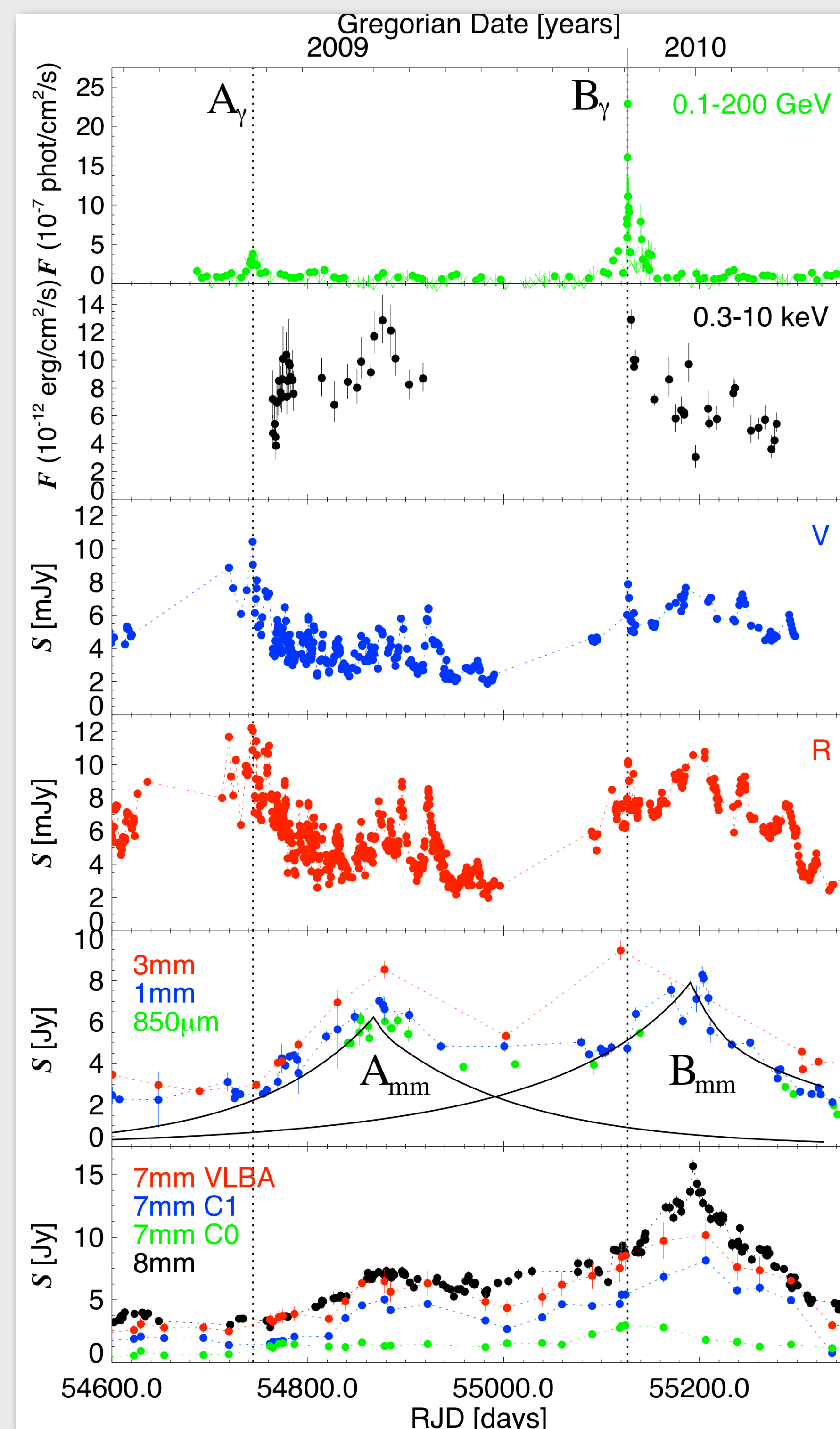


Figure 2. Light curves of OJ287 from millimeter wave to γ -ray frequencies. The vertical lines denote the times of peak γ -ray flux of A_γ and B_γ . The solid lines in the next-to-last panel represent fits to the two major 1 mm flares by using the method of Chatterjee et al. (2008). RJD = Julian Date $-2,400,000.0$. Reproduced from Agudo et al. (2011)

Variability of Linear Polarization

C0 and C1 dominate the evolution of the linear polarization p and electric-vector position angle χ at 7mm in OJ287 (Fig. 3). Whereas $p_{C0} > 10\%$, C1 exhibits the two largest peaks in p ever observed in OJ287 at 7mm, ($p_{C1} \approx 14\%$ and 22% in the end of 2008 and 2009 resp.). Moreover, these two p_{C1} maxima are contemporaneous with A_γ and B_γ , with essentially simultaneous with the highest p_{C1} peak. *The coincidence of the strongest γ -ray outburst, and exceptionally strong polarization in C1 identifies this feature >14 pc from the central engine as the site of the variable γ -ray emission.*

The optical polarization peaks at essentially the same time as p_{C1} at 7 mm during flare B_γ . During both A_γ and B_γ , $p_{opt} \approx 35\%$, which requires a well-ordered magnetic field. The shorter timescale and larger amplitude of variability of optical polarization, as compared with those at millimeter wavelengths, are consistent with frequency dependence in the turbulence model of Marscher & Jorstad (2010).

The optical and millimeter-wave linear polarization position angle is stable at $\chi \approx 160^\circ$ – 170° —similar to the structural position angle of the inner jet—both near A_γ and B_γ and throughout most of the monitoring period. The corresponding direction of the magnetic field is transverse to the direction between features C0 and C1.

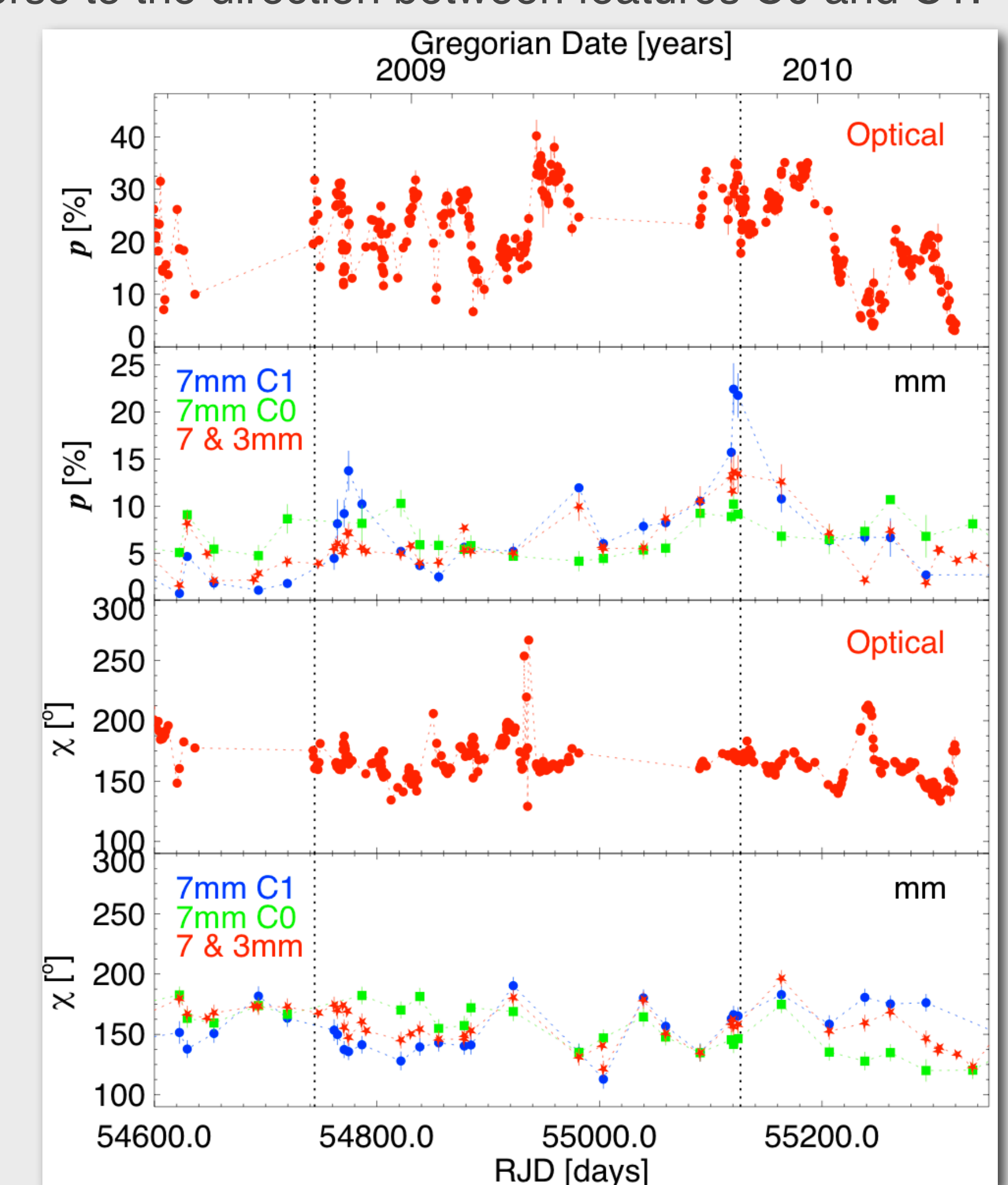


Figure 3. Optical and millimeter-wave linear polarization of OJ287 as a function of time. The optical data includes R-band and 5000–7000 Å observations. The similarity of the integrated linear polarization at 7 mm and 3 mm also allows us to combine them. Vertical lines are as in Figure 2. Reproduced from Agudo et al. (2011).

Low Probability of Chance Coincidences

The probability that a γ -ray outburst occurs by chance during the rise of a 1mm flare is only 17%. Hence, the probability that two γ -ray flares at random times occur by chance during the rising phase of two millimeter-wave flares is 3%, i.e., events A_{mm} and B_{mm} are associated with A_γ and B_γ , respectively, at 97.0% confidence level. This rises to 99.2% if, instead of A_{mm} and B_{mm} , the two high p_{C1} millimeter-wave peaks are considered.

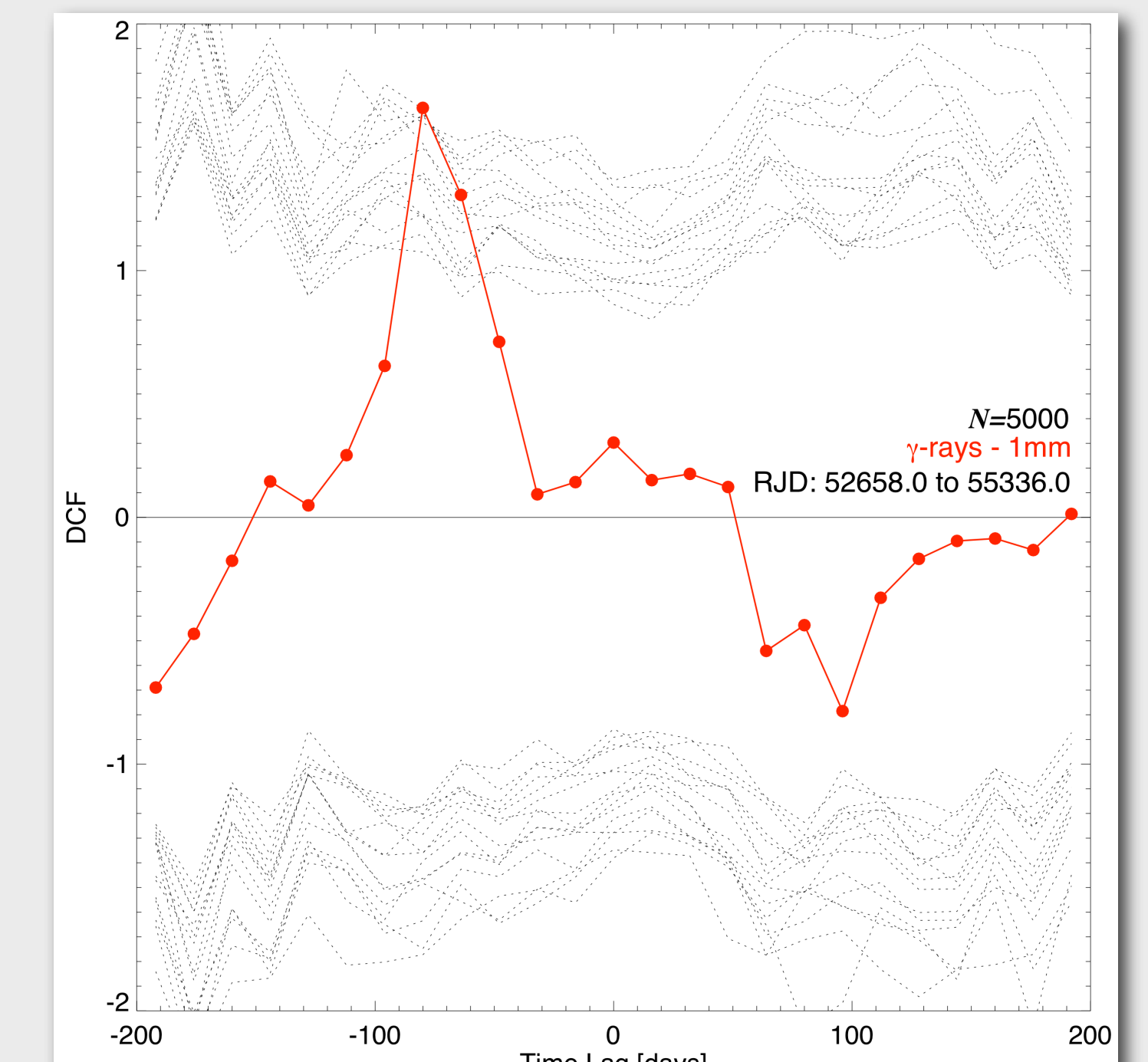


Figure 4. Discrete cross-correlation function between the γ -ray and 1 mm light curves of OJ287 (red points). The dotted curves at positive (negative) DCF values denote 99.7% confidence limits for correlation rather than stochastic variability. Reproduced from Agudo et al. (2011).

The observational evidences

We find that two kinds of events at millimeter wavelengths are related to the two reported γ -ray outbursts at high significance: (1) the early, rising phases of the two most luminous 1 mm flares ever detected in this blazar (A_{mm} and B_{mm}) and (2) two sharp increases to unprecedented levels of linear polarization ($\sim 14\%$ and $\sim 22\%$) in bright jet feature C1 > 14 pc from the central engine. These events also coincide with: (3) two sharp optical flares, (4) two peaks in optical polarization of $\sim 35\%$, and (5) the similarity of optical and millimeter-wave polarization position angle both during and between the flares at $\chi \approx 160^\circ$ – 170° .

The exceptionally high polarization of C1 during γ -ray flare B_γ provides extremely strong evidence that the event occurred in C1.

Conclusions

We propose a scenario in which the optical and γ -ray flares are produced in C1 by particle acceleration in a moving blob when it crosses a standing shock (Fig. 5) well beyond the acceleration and collimation zone (ACZ). D’Arcangelo et al. (2007) associated the innermost millimeter-wave jet emission feature with a conical shock at the end of the ACZ. We identify C0 as such a feature, and C1 as a second conical shock, as seen in hydrodynamical simulations. The blob needs to be composed of turbulent plasma given the typical weakness of the observed polarization outside the high p peaks.

The linear polarization model of Cawthorne (2006) for the polarized emission of a blob crossing a conical standing shock reproduces the observed polarization behavior during both A and B flares.

In general, the γ -ray IC emission arises from either the synchrotron self-Compton (SSC) process or IC scattering of infrared radiation from a hot, dusty torus of size ~ 10 pc (IC/dust). An SSC model is possible given the low ratio of γ -ray to synchrotron luminosity between 10^{14} and 10^{15} Hz (≈ 2) in OJ287. However, infrared emission from the dusty torus has not been detected thus far in BL Lac objects such as OJ287.

Also, the observed quenching of the optical flares is consistent with increasing SSC energy losses (not possible in the C/dust scenario). Hence, the multi-frequency behavior of the flares is difficult to reproduce in the IC/dust model. We thus favor the SSC mechanism.

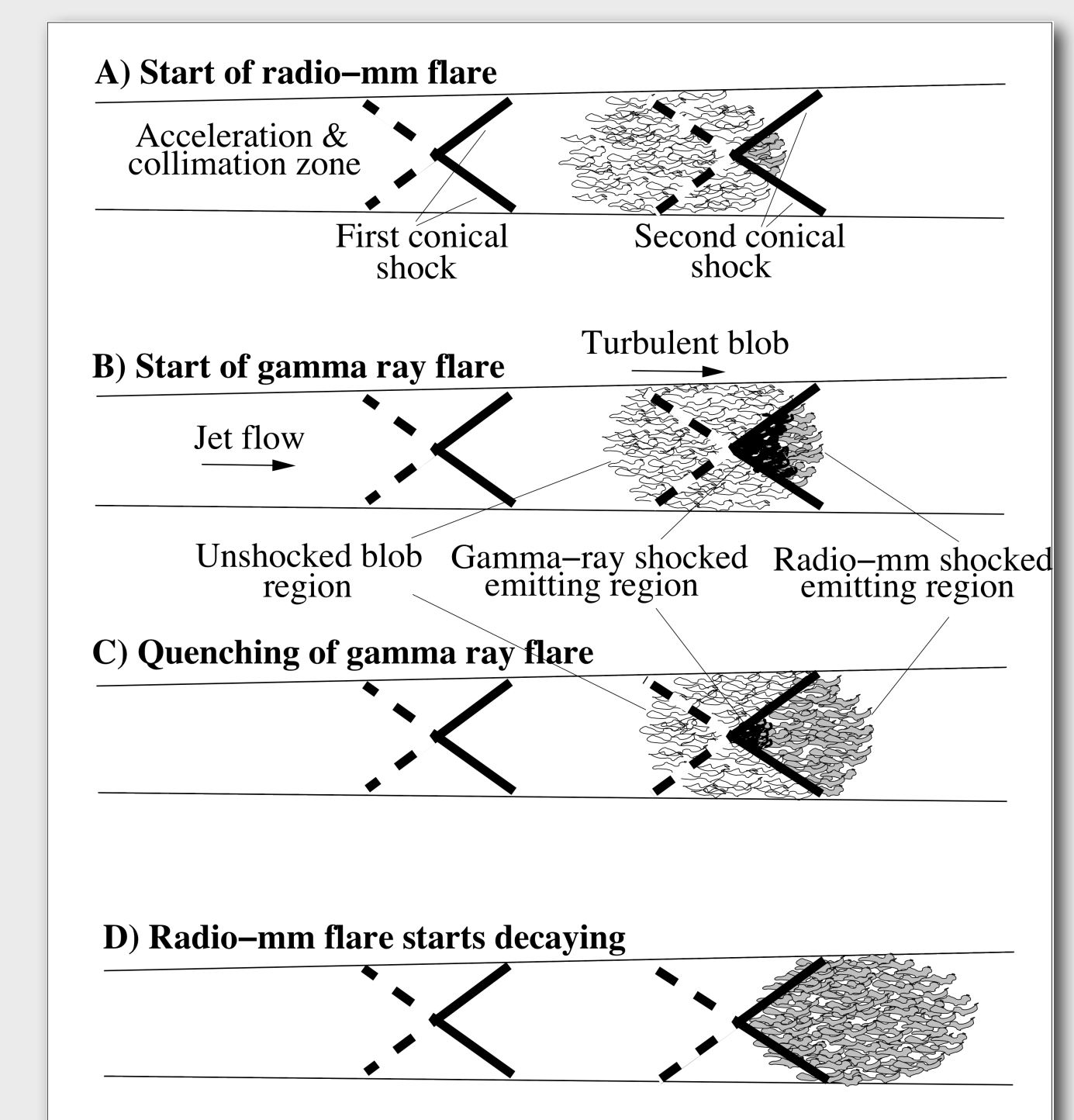


Figure 5. Sketch of proposed model for the multi-wavelength flaring behavior of OJ287. From Agudo et al. (2011).

References

Agudo, I., et al. 2011, ApJL, 726, L13
 Cawthorne, T. V. 2006, MNRAS, 367, 851
 D’Arcangelo, F. D., et al. 2007, ApJ, 659, L107
 Jorstad, S. G., et al. 2005, AJ, 130, 1418
 Jorstad, S. G., et al. 2007, AJ, 134, 799
 Marscher, A. P., & Jorstad, S. G. 2010 (arXiv: 1005.5551)
 Pushkarev, A. B., et al. 2009, A&A, 507, L33
 Villforth, C., et al. 2010, MNRAS, 402, 2087

Questions about this poster? look for me at this conference, or write me at iagudo@iaa.es

